Spatial Distributions of Solar Energetic Particles in the Inner Heliosphere

Donald V. Reames[1], Chee K. Ng[2, 3], and Allan J. Tylka[3]

[1] *Institute for Physical Science and Technology,University of Maryland, College Park, MD 20742-2431*, *dvreames@umd.edu*

[2] *College of Science, George Mason University, Fairfax, VA 22030,* cng2@gmu.edu

[3] *Space Science Division, Naval Research Laboratory, Washington, DC 20375,* allan.tylka@nrl.navy.mil

Abstract We study the spatial distribution of solar energetic particles (SEPs) throughout the inner heliosphere during six large SEP events from the period 1977 through 1979, as deduced from observations on the *Helios 1* and *2*, IMP 7 and 8, ISEE *3*, and *Voyager 1* and *2* spacecraft. Evidence of intensity maxima associated with the expanding shock wave is commonly seen along its central and western flanks, although the region of peak acceleration or "nose" of the shock is sometimes highly localized in longitude. In one event (January 1, 1978) a sharp peak in 20-30 MeV proton intensities is seen more strongly by *Voyager* at ~2 AU than it is by spacecraft at nearby longitudes at ~1 AU. Large spatial regions, or "reservoirs," often exist behind the shocks with spatially uniform SEP intensities and invariant spectra that decrease adiabatically with time as their containment volume expands. Reservoirs are seen to sweep past 0.3 AU and can extend out many AU. Boundaries of the reservoirs can vary with time and with particle velocity, rather than rigidity. In one case, a second shock wave from the Sun reaccelerates protons that retain the same hard spectrum as protons in the reservoir from the preceding SEP event. Thus reservoirs can provide not only seed particles but also a "seed spectrum" with a spectral shape that is unchanged by a weaker second shock.

Keywords: Solar energetic particles, shock waves, coronal mass ejections

1. Introduction

The most intense solar energetic-particle (SEP) events are produced by fast shock waves driven out from the Sun by coronal mass ejections (CMEs) (e.g. Reames 1990, 1995, 1999, 2002, 2009ab; Kahler 1992, 1994, 2001; Gosling 1993; Lee 1997, 2005; Tylka 2001; Gopalswamy *et al.* 2002, Ng, Reames, and Tylka 2003; Tylka *et al.* 2005; Tylka and Lee 2006; Ng and Reames 2008; Reames 2009a,b; Sandroos and Vanio 2009; Roulliard *et al.* 2011). In the largest of these events, the intensities of GeV protons are even sufficient to produce a radiation cascade that penetrates the Earth's atmosphere to be measurable by neutron monitors at ground level. Seventy of these ground-level events (GLEs) have been identified since 1942 (Cliver *et al.* 1982; Cliver 2006) of which 16 occurred during the last solar cycle (Solar Cycle 23). Energetic SEP events are of

significant practical importance since they can present a serious radiation hazard to astronauts and equipment in space and even to the passengers and crew on commercial aircraft flying polar routes.

For most of the GLEs since the 1970's there have been fairly complete measurements of particle energy spectra, time histories, element abundances, and angular distributions from satellites near Earth, so we no longer need to rely on indirect measurements of secondary radiation at ground level. However, GLEs still form an interesting and important class of events. GLEs originate from an extremely wide band of solar longitudes, approaching ~180°, suggesting an extensive spatial distribution of the particles across the broad front of the shock. In a few cases we have been fortunate enough to measure the events on multiple spacecraft distributed across the inner heliosphere, so we can better define the regions of peak acceleration and follow the spread of the particles in space and time (e.g. Reames, Barbier, and Ng 1996; Reames, Kahler, and Ng 1997; Reames 2010; Rouillard *et al.* 2011). The temporal pattern of SEP intensity at a given spacecraft depends markedly on its location relative to that of the source of the CME that drives the shock wave, and this pattern is skewed by the spiral interplanetary magnetic field. The generally accepted spatial pattern of SEP events is as follows (Reames, Barbier, and Ng 1996; Reames 1999): A spacecraft at longitudes to the east of the shock source is magnetically connected to the powerful nose of the shock early in the event when it is near the Sun and the acceleration is strongest, but intensities then decline as the magnetic connection point moves eastward along the flank of the expanding shock. A spacecraft observing at the same longitude as the source is best connected later in the event when the nose of the shock passes over it and an intensity peak is often seen. A spacecraft to the west of the source begins to see particles when it first becomes connected to the weak western flank of the shock, then intensities slowly rise until the expanding shock is well past and the spacecraft encounters field lines that connect it to the nose of the shock from behind.

Behind the shock, in many events, lies a region in which SEPs are quasi-trapped between the shock and the Sun, forming a large region with nearly uniform intensities. McKibben (1972) first noted nearly equal intensities of ~20 MeV protons spanning ~180° in solar longitude late in SEP events, as observed near 1 AU by the *Interplanetary Monitoring Probe (*IMP*) 4* and the *Pioneer 6* and

7 spacecraft. Twenty years later, Roelof *et al.* (1992) observed extended periods in the decay phase of large SEP events when intensities of both low-energy electrons and ions were the same at *Ulysses* at 2.5 AU as they were at the IMP 8 near Earth. They described the region of containment between the magnetic structures created behind one or more SEP events and the Sun as an SEP "reservoir." Subsequently, Reames, Kahler, and Ng (1997) studied the "invariant spectral region" behind large SEP events comparing proton spectra between ~1 and ~100 MeV on *Helios 1*, *Helios 2*, and IMP 8. They found nearly identical intensities and spectra spanning regions as large as 160° in solar longitude, implying significant eventual cross-field transport at all energies to produce the extreme uniformity. The spectra maintained their shape but decreased in overall intensity with time as the "magnetic bottle" containing them expanded adiabatically. Recently, Tylka *et al.* (2012) found detailed agreement in comparing the spectra of the elements from He through Fe in reservoir regions observed by *Ulysses* at 2.54 AU with those observed near Earth on the *Wind* and *Advanced Composition Explorer,* ACE, spacecraft. In addition to trapping of SEPs downstream of the shock that accelerates them, particles streaming upstream of a new shock source near the Sun are sometimes seen to be reflected and returned as a beam from structures beyond 1 AU (Tan *et al.* 2008, 2009).

These observations of reservoirs raise serious questions about trapping and the ease of particle transport across magnetic fields. Upstream of shock waves there can be strong longitudinal gradients in SEP intensities that indicate gradients in acceleration along the shock and a minimum of cross-field transport (e.g. Reames, Barbier, and Ng 1996; Reames, Kahler, and Ng 1997). Even stronger evidence of a lack of cross-field transport comes from observations of strong intensity variations early in impulsive SEP events by Mazur *et al.* (2000). Here particles were seen on some flux tubes that connected to the impulsive solar source but were absent on neighboring flux tubes that did not. These particles seemed unable to cross onto neighboring field tubes while traveling out to 1 AU. In striking contrast, however, we also see anomalous cosmic rays from the outer heliosphere that have penetrated uniformly inside well-defined magnetic clouds that were once considered to be closed magnetic structures (Reames, Kahler, and Tylka 2009; Reames 2010). We also see SEPs uniformly spanning ~160° of solar longitude in reservoirs late in SEP events. To what extent are particles contained

by magnetic fields and how do they sometimes spread with complete uniformity across the face of the Sun?

During the period from late 1977 to the middle of 1979, a unique armada of spacecraft plied the inner heliosphere and several GLEs and other large SEP events occurred. IMP *7* and *8,* located near Earth, were later joined by the *International Sun-Earth Explorer,* ISEE *3*, while *Helios 1* and *2* were well-separated in the region between 0.3 and 1 AU, and *Voyager 1* and *2* were moving outward from 1 to ~5 AU. While a few of the SEP events in this period have been studied previously, many have scarcely been examined at all, and the inclusion of data from all available spacecraft has been rare. In this paper we undertake a multi-spacecraft study of large SEP events during this time period in an effort to improve our understanding of the distribution and strength of acceleration along the shock surface and of the spatial and temporal evolution of reservoirs.

Note that for typical near-Earth observations one would usually say that an SEP source is to the west (of the observer), for example W50 on the Sun. However, for multi-spacecraft observations, the source must become the reference and we say that the same observer is to the east (of the source). This reversed reference allows us to compare many observers for a single source, although we continue to give flare and source longitudes relative to Earth, as is customary.

2. OBSERVATIONS

We consider, in time order, those large SEP events during our study period where the spacecraft are distributed so as to provide new spatial information on acceleration or on the formation and distribution of a reservoir. For study, we require that events be observed at three or more well-separated locations and show evidence of >100 MeV protons at one or more locations. Events that are obviously complicated by multiple SEP injections have been excluded. We consider protons over a broad energy range and we also include 4-8 MeV electrons in an attempt to separate the effects of rigidity and velocity. Only relativistic electrons can interact with Alfvén waves as the protons do.

2.1 The Events of September 19 and 24, 1977

We first consider the events of September 19 and 24, 1977 shown in Figures 1 and 2, respectively. Both events are GLEs at Earth. The upper panels of the

figures show the configuration of the spacecraft relative to the probable direction of emission of the CME, as derived from the longitude of the associated Hα flare, that is shown as downward in this and subsequent figures. The nominal magnetic field line from each spacecraft is calculated from the locally observed solar wind speed at the event onset. The lower panels in the figures show a comparison of the intensity-time profiles at each spacecraft for protons of three energies and for electrons of a single energy. The time of the peak of the associated Hα flare at the Sun is shown by a vertical line in the lower panels labeled by the flare longitude as observed from Earth (IMP 8). Other vertical lines mark the times of passage of shock waves, labeled by the observing spacecraft.

Helios 1 and *2* are located at 0.65 and 0.70 AU, respectively, on the 19th and at 0.60 and 0.66 AU on the 24th. Data from *Voyager* have been omitted during these events since the *Voyager* spacecraft are still quite near IMP 8 and provide no significant new information. The configuration of the spacecraft is similar in these two events, the greatest difference being the longitude of the CME source, W57 on the 19th and W120 on the 24th.

IMP 8 is magnetically well connected to the source early in the GLE event on September 19, and the intensities at all energies rise rapidly as shown in Figure 1. The intensities at the poorly connected *Helios* spacecraft rise slowly and, at *Helios 1*, the low-energy protons reach maximum intensity after the passage of a double shock. Above 20 MeV, proton intensities show evidence of a reservoir lasting ~2 days, but the 6-11 MeV protons show only a late merging at *Helios 1* and *2* while intensities at IMP 8 follow a similar trajectory of decline as *Helios 1*, but with a reduced intensity at these low energies. The electron channel shows little increase at *Helios*, and at all spacecraft the electrons return to instrument background, which is different for *Helios* and IMP*8*, during September 22 and 23.

The particle onsets in the GLE of September 24, shown in Figure 2 (also at the end of Figure 1) are quite surprising. Intensities of each species shown rise rapidly at *Helios 1* and IMP 8 to very similar values, even though the spacecraft are separated by 145^{o} in longitude. Meanwhile, intensities at *Helios 2*, only 24^{o} to the west of *Helios 1*, show a very slow rise. These observations appear to suggest a wide strong shock similar, in some sense, in the directions of *Helios 1* and IMP 8, but weakening greatly in the direction of *Helios 2*. The presence of particles in the reservoir behind the event of September 19 may well contribute to the seed

population for shock acceleration on September 24. We will discuss this possibility in detail in Section 3.3.

Later in the event of September 24 we see intensity peaks occurring shortly after the times of shock passage at *Helios 1* and somewhat later at *Helios 2* (see Figure 2). A reservoir, involving all three spacecraft, forms on September 25 for electrons and high-energy protons and on September 26 for 20-30 MeV protons. A reservoir may also form for 6-11 MeV protons spanning *Helios 1* and *Helios 2*, but intensities at IMP 8 are much lower, as they were during the reservoir period for the September 19 event. The spatial extent and filling time of a reservoir seems to depend inversely upon particle velocity in this event and in others studied below. The rapid reservoir formation for electrons suggests that velocity, not rigidity, is the appropriate variable.

2.2 The Event of January 1, 1978

Observations of the event of January 1, 1978 are shown in Figure 3. This event, observed from Earth at E6, is not a GLE. However, *Helios 1*, at 0.95 AU and 38^{o} to the east of Earth sees quite high intensities of energetic protons. If Earth had been located at the longitude of *Helios 1*, the event would likely have been observed at ground level. For proton energies <30 MeV, IMP 8 and *Helios 2* (0.93 AU) nearby, both see intensity maxima shortly after local shock passage.

As in the previous events, evidence of a reservoir is seen at different times for different energies in this event. For electrons and for protons >100 MeV, equal intensities at *Helios 1*, *Helios 2*, and IMP 8 are seen beginning about midday on January 2. For protons <30 MeV, all four spacecraft have comparable intensities beginning midday on January 4.

Most unusual in this event is the sharp intensity peak at energies below ~30 MeV at the time of shock passage at *Voyager* (note that *Voyager 1*and *2* are quite close together and only data from *Voyager 2*, at 1.95 AU, are shown). Particles ~20-30 MeV that are accelerated early by the shock when it was at the base of the field line to *Voyager* only begin to arrive about a day after the event onset, early on January 3. However, 4 days after the onset, the shock itself arrives at *Voyager* and is still accelerating protons up to ~30 MeV locally, producing the peak. This point on the shock has passed between *Helios 1* and *Helios 2* to arrive at *Voyager* at 1.95 AU, following the dashed path shown in the upper panel of Figure 3. At

low energies, the shock peak at *Voyager* is just as intense as it was at *Helios 2* and IMP 8.

2.3 The Event of April 28, 1978

Figure 4 shows observations during the event of April 28, 1978. *Helios 1* and *2* are each near perihelion at 0.31 and 0.29 AU, respectively, during this event, and *Voyager 2* is at 2.93 AU. IMP 8 views the event at E38 on the Sun and a GLE is not seen. Despite its distance, *Voyager 2* sees a strong increase in >100 MeV protons early, and at lower energies with an increasing delay.

However, the most striking feature of this event is the peak in intensity, especially seen at *Helios 2* for electrons and all energies of protons just after passage of the shock. Figure 5, at an expanded time scale, compares peaks in the particle intensities for three spacecraft with corresponding peaks that are found in the solar wind speed at times labeled A, B, and C in the upper panel. In Figure 6, a comparison of the proton spectra at these three times shows considerable similarity. This suggests that a reservoir, formed very early behind the shock is seen as it passes *Helios 1* (at 0.31 AU), is glimpsed briefly as the west flank passes *Helios 2*, and finally arrives at IMP 8.

It is surprising that the reservoir seen by *Helios 1* and *2*, near 0.3 AU, appears with nearly the same intensity at IMP 8, near 1 AU, more than a day later. We might have expected the intensity to fall as the reservoir expands. Evidently the shock continues to add SEPs, to approximately compensate for the expansion, all the way to 1 AU.

Helios 1 and IMP 8 appear to remain embedded in the reservoir after each encounters it, but *Helios 2* detaches from it after crossing the high-speed solar-wind region. To understand this we appeal to the CME simulations of Manchester *et al.* (2005) and especially consider the north-south solar-wind speed profile in their Figure 3a. In this simulation, the CME is emitted at the solar equator, while our April 28 event occurred at 22N so that the southern tip of the high-velocity distribution might pass *Helios 2* which also passes nearest the western boundary of the shock. Thus *Helios 2* briefly samples field lines deformed by the high-speed region that connect to the stronger shock above.

2.4 The Event of September 23, , 1978.

The large GLE of September 23, 1978 is shown in Figure 7. Although this event was studied by Reames, Kahler, and Ng (1997), here we also show electrons, >100 MeV protons, and observations from *Voyager*. Since the solar wind speeds differ at *Voyager 1* and *2*, we show magnetic field lines from both spacecraft. However, comparison of these two field lines mainly shows the error in constant-velocity extrapolation from such a great distance. *Voyager 1* and *2* are at 4.2 and 3.9 AU, respectively; *Helios 1* and *2* are at 0.76 and 0.74 AU, respectively.

A reservoir encompassing *Helios 1* and IMP 8 forms for all species after the shock passes IMP 8; *Helios 2* probably enters this reservoir shortly thereafter. At the *Voyager* spacecraft, despite their distance, the intensities of 22-27 MeV protons reach the reservoir value by September 28 and protons at lower energies are still rising toward the reservoir value during that time. This uniform reservoir has spread far out into the heliosphere.

2.5 The Event of March 1, 1979.

The event of March 1, 1979 is shown in Figure 8. This event was also studied by Reames, Kahler, and Ng (1997) and by Reames (2010) but we have expanded the coverage here. *Helios 1*, *Helios 2*, and *Voyager 2* were at 0.95, 0.93, and 4.76 AU, respectively, during this event.

Voyager sees an early increase in protons at >100 and at ~20 MeV in response to early proton acceleration at the base of its field line (despite the apparently poor connection). In the inner heliosphere, a reservoir forms for electrons and for ~20 MeV protons involving *Helios 1*, *Helios 2*, and IMP 8 on March 3. However, 6-11 MeV protons do not appear to join the reservoir until midday on March 4.

3. DISCUSSION

3.1 SEP Intensity Distributions along the Shock

The highest SEP intensities and the hardest energy spectra are usually seen early on the east flank of the event where an observer is magnetically connected to the distant nose of the shock when it is still close to the Sun and at its strongest. The SEPs are swept to the east by the spiral magnetic field lines from the rotating

Sun. However, near the shock nose, and along its west flank, particles up to ~30 MeV frequently peak at or behind the shock. These shock-associated peaks are common and can be quite dramatic, especially when the observation is made well inside 1 AU. A lack of observed shock-associated peaks in a large SEP events generally means that the spacecraft are not favorably located. This is true of the GLE of November 22, 1977 reported recently by Reames and Lal (2010) where all 6 spacecraft encounter the shock on its eastern flank and none see peaks at the time of shock passage. We have not repeated observations from this event here.

The point of maximum acceleration along the shock front can be highly localized. If an observing spacecraft does not cross the shock at the correct longitude, the peaks are weak or may fall appreciably behind the shock. A striking example is the event of January 1, 1978 (Figure 3), where *Voyager*, despite its distance of 1.95 AU, sees a sharp shock peak, while *Helios 1*, 16.3° to the east, and *Helios 2*, 17.8° to the west, (both near 1 AU) see no sharp peaks at the time of shock passage. *Helios 1* sees a typical profile of the eastern flank that peaks early and decreases behind the shock, while *Helios 2* sees a rounded peak well behind the shock. In this event *Voyager* is 16° to the east of the flare longitude, so we cannot assume that the "nose of the shock" defined by maximum acceleration necessarily coincides with the flare longitude. However the peak at *Voyager* is probably aided by the fact that the shock is more likely to be quasi-perpendicular as the Parker spiral winds more tightly farther from the Sun.

Two other events show sharp intensity peaks just after the time of shock passage: in the March 1, 1979 event (Figure 8) *Helios 1* is 9° to the east of the flare longitude, and in the September 24, 1977 event (Figure 2) *Helios 1* is 25° to the west of the flare longitude. Thus the flare longitude may only be an approximation to the point of maximum acceleration along the shock. This situation is further complicated by the fact that CMEs may be emitted ~20° above or below the ecliptic so that the point of maximum particle acceleration might lie above or below the observer. However, in most large SEP events, spacecraft passing through the western flank of the shock will see some vestige of the intensity peak at the shock nose, even when the nose itself is not directly encountered.

3.2 Reservoirs

Most large SEP events have large regions of space, occurring late in the event, where there is little or no spatial gradient in the intensities of particles in longitude, latitude, or radius. Within these regions the energy spectral shapes are invariant in space and time with the overall intensity decreasing with time as the volume of the containment region increases. What we can see in this study is that the boundaries of the invariant reservoir can depend upon energy and time. For example, in the September 24, 1977 event (Figure 2), for electrons and for >100 MeV protons, the three spacecraft reach the same intensities early on September 25th, for ~20-30 MeV protons the same intensities are obtained at about 8 UT on the 26th, and 6-11 MeV protons, the intensity at IMP 8 tracks below that on *Helios 1* and *2* indefinitely. In the March 1, 1979 event (Figure 8), the electrons and the ~20-30 MeV protons (also presumably the >100 MeV protons) have formed a reservoir by ~12 UT on March 3. However, at 6-11 MeV, *Helios 1* and *2* form a reservoir at about the same time, but IMP 8 does not join them for ~24 hrs.

Electrons of 4 MeV have a rigidity of 4.5 MV while a 6 MeV proton has a rigidity of 106 MV, so the electrons have rigidities well below those of any of the protons we have considered. However, the electrons are relativistic and they behave like the higher energy protons in terms of reservoir formation. Thus the spread of particles throughout a reservoir appears to depend much more on particle velocity than rigidity. This tends to support a model in which particles must wander throughout a maze of tangled magnetic field lines (*e.g.* Reames 2010) produced by the random walk of their foot points in the photosphere (Jokipii and Parker 1969; Parker 1987). The time required to follow a long torturous path leading to a remote solar longitude depends upon the particle velocity.

Furthermore, during long periods of reservoir observation, the decay time for various species and energies track each other, showing no rigidity dependence. Protons of >100 MeV do not leak from the reservoir any more rapidly than those of a few MeV. This was shown for various energy protons by Reames, Kahler, and Ng (1997); here we see that electrons also follow this pattern. The decay is controlled by adiabatic expansion of the volume of the entire reservoir structure, not by differential leakage of different species or rigidities.

The enhanced magnetic field and waves/turbulence a short distance behind the shock constitute a very effective trap. To escape, the particles have to be scattered through the loss cone associated with the enhanced field, but first they have to fight the intense scattering to get to the magnetic bottle neck and then have to be scattered into the loss cone to escape upstream. This greatly reduces the likelihood of escape for particles in the energy range we observe. On the other hand, the particles have easy transport within the trap which tends to flatten the spatial gradient (see Ng, Reames, and Tylka 2003, Figure 2).

In some cases the reservoir is ephemeral. In the event of April 28, 1978 (Figures 4, 5, and 6) we had to compare the energy spectra to identify the reservoir being convected past each spacecraft. Here the correlation of the intensities with the high-speed solar wind led to reservoir identification. However, this is the only event for which we can correlate the reservoir with the solar wind speed; it is also a rare event where the *Helios* spacecraft are unusually close to the Sun.

Early multi-spacecraft studies sometimes reduced their observations to plots of maximum proton intensity as a function of spacecraft longitude relative to the source. They tried to explain these plots as Gaussian in form, that might result from cross-field "coronal" diffusion of the particles (*e.g*. Lario *et al.* 2006). However, such plots completely obscured the existence of a reservoir. In fact, in Figure 8 we see an example where the 6-11 MeV protons at *Helios 2* and at IMP 8 peak when each spacecraft enters the reservoir. The difference in these two peak intensities is entirely explained by the volume expansion of the reservoir between the times that the two spacecraft enter it; this is a variation in time, definitely not a gradient in space. The volume expansion of the reservoir in time has nothing whatever to do with lateral diffusion of particles. However, the random walk of the field lines does permit a form of field-line diffusion that results in a network through which the particles eventually flow, beginning from their spatially non-uniform source distributed along the shock.

The lateral width of the reservoir is not necessarily the same for all species and energies. It depends upon the width of the shock, the turbulence of the pre-existing magnetic field, and the velocity of the particles.

To what extent are SEPs bounded by magnetic fields? This important question has an imprecise answer. Evidence that particles do not easily cross the magnetic fields is as follows:

(1) During transit of 1 AU, particles from a point source cannot cross onto neighboring flux tubes that do not intercept the source (Mazur *et al.* 2000).

(2) Significant spatial gradients are seen far upstream of shocks when the particles can escape freely (e.g. Figures 7 and 8)

(3) The existence of reservoirs with spectral invariance shows there is enough trapping along field lines that high-energy particles do not escape reservoirs more rapidly than low-energy particles.

Evidence that particles can easily cross field lines is as follows:

(1) Anomalous cosmic rays (*e.g*. ~4 MeV/amu He) are seen uniformly throughout CMEs and magnetic clouds at solar minimum (Reames, Kahler, and Tylka 2009).

(2) The frequent uniformity of particles of all species and energies in the interior of reservoirs shows that cross-field transport can occur given sufficient trapping for a sufficient time.

Particles can often traverse large regions of space when given sufficient time. Even protons of 6 MeV travel 20 AU/day probing for magnetic pathways leading to distant longitudes. Thus, cross-field transport occurs after significant periods of time. However, there are also events like the "delayed proton event" of June 5, 1979 (see Reames, Barbier, and Ng 1996) where no particles arrive at IMP 8 for more than a day after the event onset when the shock suddenly intercepts the field line to Earth. Of course, this shows that it is essential that the shock reach the field line to the observer (see also Rouillard *et al*. 2011)

3.3 Seed Population

To some degree, particles observed late in one SEP event, as in the reservoir behind that event, are likely to contribute to the seed particles available for acceleration in a subsequent event (*e.g*. Desai *et al.* 2003). Suprathermal or energetic particles from an earlier event are more easily accelerated than are thermal ions from the solar wind, especially in a quasi-perpendicular shock wave (see Tylka and Lee 2006). The question of a seed population is usually addressed by studying element or isotope abundances (Mason, Mazur, and Dwyer 1999; Desai *et al*. 2003; Tylka *et al.* 2005; Tylka and Lee 2006) and it has been

suggested that particle acceleration is enhanced by the presence of a previous SEP event (Kahler 2001; Gopalswamy *et al.* 2002; Cliver 2006). Here we consider the possible effects of spatial transport and reservoirs on the availability and injection of what might be called a "seed spectrum" of particles, for an event such as September 24, 1977.

The re-acceleration of a power-law spectrum is an example of the classical multiple-shock problem (*e.g.* Axford 1981; Melrose and Pope 1993). The distribution function $f(p)$ of accelerated particles downstream of the shock with compression ratio r is

$$f_a(p) = ap^{-a}\int_0^p dq\; q^{a-1}\Phi(q) \qquad (1)$$

where $a=3r/(r-1)$ and $\Phi(p)$ is the injected distribution. If $\Phi(p)= k\,\delta(p-p_0)$, then

$$f_a(p) = \frac{ak}{p_0}\left(\frac{p}{p_0}\right)^{-a} \quad \text{for } p>p_0, \quad f_a(p) = 0 \text{ for } p<p_0 \qquad (2)$$

For simplicity we neglect adiabatic decompression of this first population that would reduce the overall intensity, but not change the spectral shape.

For acceleration of this population by a second shock with compression ratio r', we set $\Phi(p) = f_a(p)$, and let $b=3r'/(r'-1)$. Integrating the power-law forms for $p>p_0$, we find

$$f_{a,b}(p) = \frac{kab}{p_0(b-a)}\left[\left(\frac{p}{p_0}\right)^{-a} - \left(\frac{p}{p_0}\right)^{-b}\right] \quad \text{for } a \neq b, \qquad (3)$$

and

$$f_{a,a}(p) = \frac{ka^2}{p_0}\left(\frac{p}{p_0}\right)^{-a}\ln\left(\frac{p}{p_0}\right) \quad \text{for } a = b. \qquad (4)$$

However there may also be acceleration from the solar wind at the second shock producing an additional contribution

$$f_b(p) = \frac{bk'}{p_0}\left(\frac{p}{p_0}\right)^{-b} \qquad (5)$$

which may or may not be significant, depending upon the values of k' and b. Finally, the intensity $j(E) = p^2 f(p)$.

From Equation (3) it is clear that the reaccelerated spectrum will be dominated by the stronger of the two shocks with the flatter spectrum. The spectra of the first and second shock appear symmetrically.

From Figure 2, it is clear that for IMP 8 and *Helios* 1, the intensities of all species shown for the September 24th event reach a plateau or peak intensity, the same for both spacecraft, several hours after the event onset and lasting ≥12 hours. This plateau intensity above 6 MeV is a factor of ~100 below the streaming limit (Reames and Ng 2010) and, hence, does not arise from excessive wave generation during transport from the shock. The particles in the September 24th event are accelerated onto the same field lines that defined the spatial region of the reservoir behind the September 19th event. Thus we can imagine that these newly accelerated particles begin to fill the same reservoir in 6-12 hours, depending on their velocity, and a balance is established between expansion and acceleration as the new shock weakens and the old reservoir expands.

Figure 9 shows the spectra at IMP 8 and *Helios 1* during the reservoir period preceding the September 24th event and on the plateau region early in the event. At high energies the plateau spectra are similar to the background spectra, especially at *Helios 1*, strongly suggesting reacceleration by a weaker secondary shock as described by Equation 3. The normalization of Equation 3 would not explain the large intensity increase in the new event; however, the equation does not consider the cumulative effects of transport and especially the trapping that probably affects the intensities we observe. The rollover of the plateau spectrum at low energies at IMP 8 may occur because Figure 9 shows fewer low-energy protons in the reservoir at IMP 8 and because these protons are less efficiently accelerated by the quasi-perpendicular shock so far around on the flank. Note that during the ~5 days between the two events, the Sun has rotated through an angle of ~65^{o}, carrying the suprathermal seed population (below the energies we cam measure) to the west, away from IMP 8 and toward *Helios*. At low energies, this rotation may exceed any cross-field lateral transport, depleting the seed population at IMP 8. In addition, it is also possible that the path length to IMP 8 is longer than the spiral path we have assumed.

At longitudes where the shock in the event of the 24th remains weaker than that on the 19th, that is $a<b$, the spatial variations in b along the shock will have little effect on the resulting spectral shape. The spatial uniformity of the resulting

accelerated spectrum derives mainly from the spatial uniformity of the pre-event reservoir. Cross-field transport of the accelerated particles early in the new event is not required. However, if $a>b$ at some longitudes, then the harder new spectrum will dominate. The spectrum of accelerated particles, especially at *Helios 1*, appears to be derived from the "seed spectrum" of the reservoir. The high-energy spectrum at IMP 8 is at least as hard. While *Helios 2* also shares the same seed population, there appears to be no acceleration early on the 24th, suggesting that the shock does not extend to the base of the field line connecting to *Helios 2*. However, by the time the shock passes *Helios 1* and *Helios 2* on September 25th (see Figure 2) the shock spectra at the 2 spacecraft are quite similar.

Acceleration of particles to produce the same spectrum as the ambient seed population has been observed *in situ* by Desai *et al.* (2004). They found many events for which the shock spectral index of Fe was correlated with that in the ambient population preceding arrival of the shock (see their Figure 12b). In some cases the ambient population is the reservoir from an earlier event (see e.g. their Figure 2). Also, shock waves weaken as they move out from the Sun, so it is not surprising that locally they encounter material that was accelerated earlier when the shock was stronger. This explains why spectra at shocks often fail to correlate with local shock parameters. When $a<b$, the observed spectral indices do not correlate with b.

4. CONCLUSIONS

We have studied the spatial distributions of protons and electrons using 7 spacecraft, usually at 4 distinct locations. When spacecraft sample the shock's central and western flank, shock-related peaks are usually seen up to ~30 MeV out to ~1 AU and, in one case, even to ~2 AU. We suggest that these shock-associated peaks are a feature of the spatial structure of large SEP events; when they are not seen it is probably because the observing spacecraft are unfavorably located. In some cases there is evidence that the region of maximum acceleration or "nose" of the shock is rather limited in longitudinal extent.

Particles accelerated by the shock feed into reservoirs or invariant spectral regions of large spatial extent behind the shock. Given sufficient time, these particles can spread longitudinally "across" magnetic field lines following paths

along field lines (Reames 2010) that are tangled by the random walk of their photospheric foot points (Jokipii and Parker 1969). Particles from the shock have no trouble entering the CME and magnetic cloud (Reames 2010) given sufficient time. Since the path length to a distant longitude may be long, particles with the highest velocity tend to fill the largest volumes first, and the reservoirs are first established by electrons and protons of the highest velocity. Eventually the spatial distribution in the reservoir can become quite uniform, decreasing its overall intensity adiabatically and maintaining spectral invariance as the volume expands. In the event of April 28, 1978 we glimpse the invariant spectral reservoir as it passes 0.3 AU, then see it later when it arrives at 1 AU with the same proton spectral shape.

Particles in the reservoir behind one shock wave form a seed population that may dominate the acceleration by a second shock. The spectral index of the final accelerated population is determined by the strongest shock with the highest compression ratio. This appears to occur when the high-energy spectra of protons accelerated by the September 24, 1977 event in the direction of *Helios 1* show a spectral index similar to those in the reservoir behind the September 19, 1977 event. Thus the harder spectrum of the seed population dominates and will prevail, even smoothing out any possible spatial variations in the compression ratio of the second shock, as long as the second shock remains weaker than the first. At longitudes where the second shock is stronger, the distribution will be promoted to a harder spectrum.

If our analysis is correct, it appears possible that a second SEP event may become a GLE solely because its shock reaccelerated the energy spectrum from the reservoir behind a previous GLE. This is a potent seed population indeed!

Work by DVR was funded in part by NASA grant NNX08AQ02G, CKN was funded by NASA grant NNX09AU98G, and AJT was supported by the Office of Naval Research and NASA DPR NNG06EC55I.

REFERENCES

Axford, W. I.:1981, *Proc. 17th Int. Cosmic Ray Conf. (Paris)* **12**, 155

Cliver, E. W.: 2006, *Astrophys. J.* **639**, 1206

Cliver, E. W., Kahler, S. W., Shea, M. A., Smart, D. F.: 1982, *Astrophys. J.* **260**, 362

Desai, M. I., Mason, G. M., Wiedenbeck, M. E., Cohen, C. M. S., Mazur, J. E., Dwyer, J. R., Gold, R. E., Krimigis, S. M., Hu, Q., Smith, C. W., Skoug, R. M.: 2004, *Astrophys. J.*, **661**, 1156

Desai, M. I., Mason, G. M., Dwyer, J. R., Mazur, J. E., Gold, R. E., Krimigis, S. M., Smith, C. W., Skoug, R. M.: 2003, *Astrophys. J.*, **588**, 1149

Gosling, J. T.: 1993, *J. Geophys. Res.*, **98**, 18937

Gopalswamy, N., Yashiro, S., Michalek, G., Kaiser, M. L., Howard, R. A., Reames, D. V., Leske, R., von Rosenvinge, T., 2002, *Astrophys. J.* **572**, L103

Jokipii, J. R., and Parker, E. N.: 1969, *Astrophys. J.* **155**, 777

Kahler, S. W.: 1992, Ann. Rev. Astron. Astrophys. **30**, 113

Kahler, S. W.: 1994, *Astrophys. J.*, **428**, 837

Kahler, S. W.: 2001, *J. Geophys. Res.* **106**, 20947

Lario, D., Kallenrode, M.-B., Decker, R. B., Roelof, E. C., Krimigis, S. M., Aran, A., Sanahuja, B.: 2000, *Astrophys. J.* **653**, 1531

Lee, M. A.: 1983, *J. Geophys. Res.*, **88**, 6109

Lee, M. A.: 1997, in: *Coronal Mass Ejections*, edited by N. Crooker, J. A. Jocelyn, J. Feynman, Geophys. Monograph 99 (AGU press), 227

Lee, M. A.: 2005, *Astrophys. J. Suppl.*, **158**, 38

Manchester IV, W. B., Gombosi, T. I., De Zeeuv, D. L., Sokolov, I. V., Roussev, I. I., Powell, K. G., Kóta, J., Tóth, G., Zurbuchen, T. H.; 2005, *Astrophys. J.* **622**, 1225

Mason, G. M., Mazur, J. E., Dwyer, J. R.: 1999, *Astrophys. J.*, **525**, L133

Mazur, J. E., Mason, G. M., Dwyer, J. R., Giacalone, J., Jokipii, J. R., Stone, E. C.: 2000, *Astrophys. J.* **532**, L79

McKibben, R. B.: 1972, J. Geophs. Res. 77, 3957

Melrose, D. B., Pope, M. H.: 1993, *Proc. Astron. Soc. Au*. **10**, 222

Ng, C. K., Reames, D. V., Tylka, A. J.: 2003, *Astrophys. J.* **591**, 461

Ng, C. K., Reames, D. V.: 2008 *Astrophys. J.* **686**, L123

Parker, E. N.: 1987, *Physics Today*, **40 (7),** 36.

Reames, D. V.: 1990, *Astrophys. J. Suppl.* **73**, 235

Reames, D. V.: 1995, *Revs. Geophys. (Suppl.)* **33**, 585

Reames, D. V.: 1999, *Space Sci. Revs.,* **90**, 413

Reames, D. V.: 2002, *Astrophys. J.* **571**, L63

Reames, D. V.: 2009a, *Astrophys. J.* **693**, 812

Reames, D. V.: 2009b, *Astrophys. J.* **706**, 844

Reames, D. V.: 2010 *Solar Phys*. **265**, 187

Reames, D. V., Barbier, L. M., Ng, C. K.: 1996, *Astrophys. J.* **466**, 473

Reames, D. V., Kahler, S. W., Ng, C. K.: 1997, *Astrophys. J.* **491**, 414

Reames, D. V., Kahler, S. W., Tylka, A, J.: 2009, *Astrophys. J.* **700**, L196.

Reames, D. V., Lal, N.: 2010 *Astrophys. J.* **723**, 550

Reames, D. V., Ng C. K.: 2010 *Astrophys. J.* **723**, 1286

Roelof, E. C., Gold, R. E., Simnett, G. M., Tappin, S. J., Armstrong, T. P., Lanzerotti, L.J.: 1992, *Geophys. Res. Lett.* **19**, 1243

Rouillard, A. C., Odstrčil, D., Sheeley, N. R., Jr., Tylka, A. J., Vourlidas, A., Mason, G., Wu, C.-C., Savani, N. P., Wood, B. E., Ng, C. K., *et al.*: 2011, *Astrophys. J.* **735**, 7

Sandroos, A., Vainio, R.: 2009 A*stron. and Astrophys*. **507**, L21

Tan, L. C., Reames, D. V., Ng, C. K.: 2008, *Astrophys. J.* **678**, 1471.

Tan, L. C., Reames, D. V., Ng. C. K., Saloniemi, O., Wang, L.: 2009 *Astrophys. J.* **701**, 1753.

Tylka, A. J.: 2001, *J. Geophys. Res.* **106**, 25333

Tylka, A. J., Cohen, C. M. S., Dietrich, W. F., Lee, M. A., Maclennan, C. G., Mewaldt, R. A., Ng, C. K., and Reames, D. V.: 2005, *Astrophys. J.* **625**, 474

Tylka, A. J., Lee, M. A.: 2006, *Astrophys. J.* **646**, 1319

Tylka, A. J., Malandraki, O. E., Dorrian, G., Ko, Y.-K., Marsden, R. G., Ng, C. K., Tranquille, C.: 2012 *Solar Phys*, in press.

Figure Captions

Figure 1. The upper panel shows the configuration of the spacecraft, *Helios 1*, *Helios 2*, and IMP 8 during the GLE on September 19, 1977 relative to the CME which is directed downward as shown by the arrow. Directions of east (E) and west (W) are shown. The lower panels compare the intensities of protons and electrons observed on the 3 spacecraft at the energies (in MeV) indicated. Note that the electron intensities on September 22 and 23 are higher at *Helios* than IMP 8 only because of higher instrument background; they do not necessarily suggest absence of an electron reservoir.

Figure 2. The upper panel shows the configuration of the spacecraft, *Helios 1*, *Helios 2*, and IMP 8 during the GLE on September 24, 1977 relative to the CME which is directed downward as shown by the arrow. The lower panels compare the intensities of protons and electrons observed on the 3 spacecraft at the energies (in MeV) indicated.

Figure 3. The upper panel shows the configuration of the spacecraft, *Helios 1*, *Helios 2*, IMP 8, and *Voyager2* during the SEP event on January 1, 1978 relative to the CME which is directed downward as shown by the arrow. (*Voyager* 1 is indistinguishably close to *Voyager* 2.) The lower panels compare the intensities of protons and electrons observed on the 4 spacecraft at the energies (in MeV) indicated. Vertical lines show times of shock passage at the spacecraft indicated. Note that the electron intensities after January 4 are higher at *Helios* than IMP 8 only because of higher instrument background; they do not necessarily suggest absence of an electron reservoir.

Figure 4. Observations during the event of April 28, 1978 are shown with features as described in Figure 3.

Figure 5. Particle intensities at *Helios 1*, *Helios 2*, and IMP 8 are shown in the upper two panels and compared with the solar wind speed in the lower panel. Peaks in the solar wind speed for the

3 spacecraft correlate with peaks in the corresponding particle intensities at times labeled A, B, and C in the upper panel.

Figure 6. Proton energy spectra are shown during high-speed solar wind periods A, B, and C (marked in Figure 5) at *Helios 1*, *Helios 2*, and IMP 8, respectively.

Figure 7. Observations during the event of September 23, 1978 are shown with features as described in Figure 3.

Figure 8. Observations during the event of March 1, 1979 are shown with features as described in Figure 3.

Figure 9. Proton energy spectra at IMP 8 (red squares) and *Helios 1* (blue circles) are compared in the reservoir region prior to the September 24, 1977 GLE (open symbols) and on the plateau region in the new GLE at 10 to 12 UT (closed symbols). The new GLE plateau spectrum at *Helios 1*, fit to a power-law, is shown as a dashed line and is also shown shifted downward for comparison with the reservoir spectra. The plateau spectrum at IMP 8 has a similar slope at high energy but rolls down at low energy.

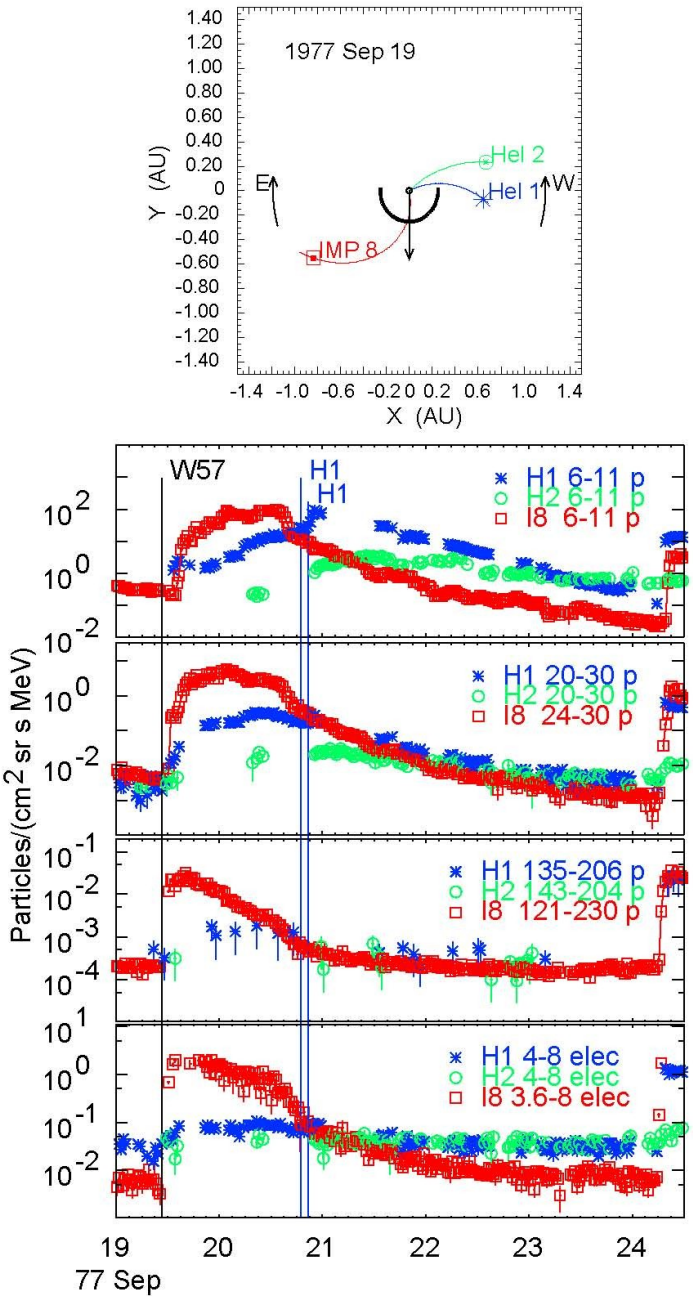

Figure 1. The upper panel shows the configuration of the spacecraft, *Helios 1*, *Helios 2*, and IMP 8 during the GLE on September 19, 1977 relative to the CME which is directed downward as shown by the arrow. Directions of east (E) and west (W) are shown. The lower panels compare the intensities of protons and electrons observed on the 3 spacecraft at the energies (in MeV) indicated. Note that the electron intensities on September 22 and 23 are higher at *Helios* than IMP 8 only because of higher instrument background; they do not necessarily suggest absence of an electron reservoir.

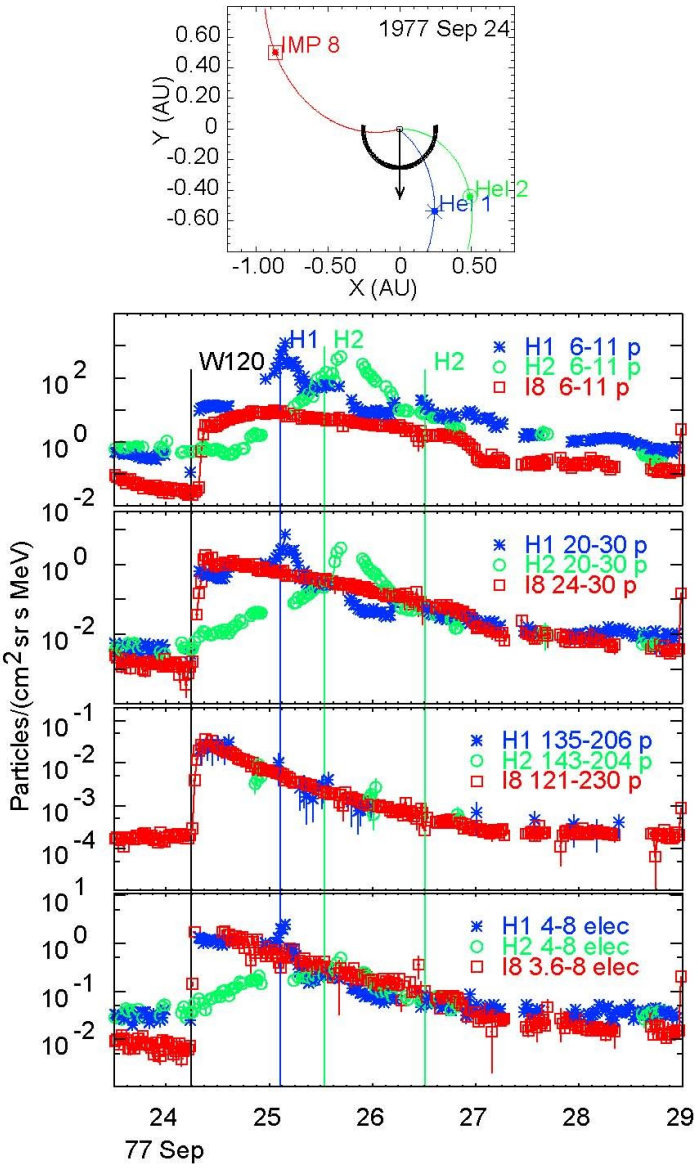

Figure 2. The upper panel shows the configuration of the spacecraft, *Helios 1*, *Helios 2*, and IMP 8 during the GLE on September 24, 1977 relative to the CME which is directed downward as shown by the arrow. The lower panels compare the intensities of protons and electrons observed on the 3 spacecraft at the energies (in MeV) indicated.

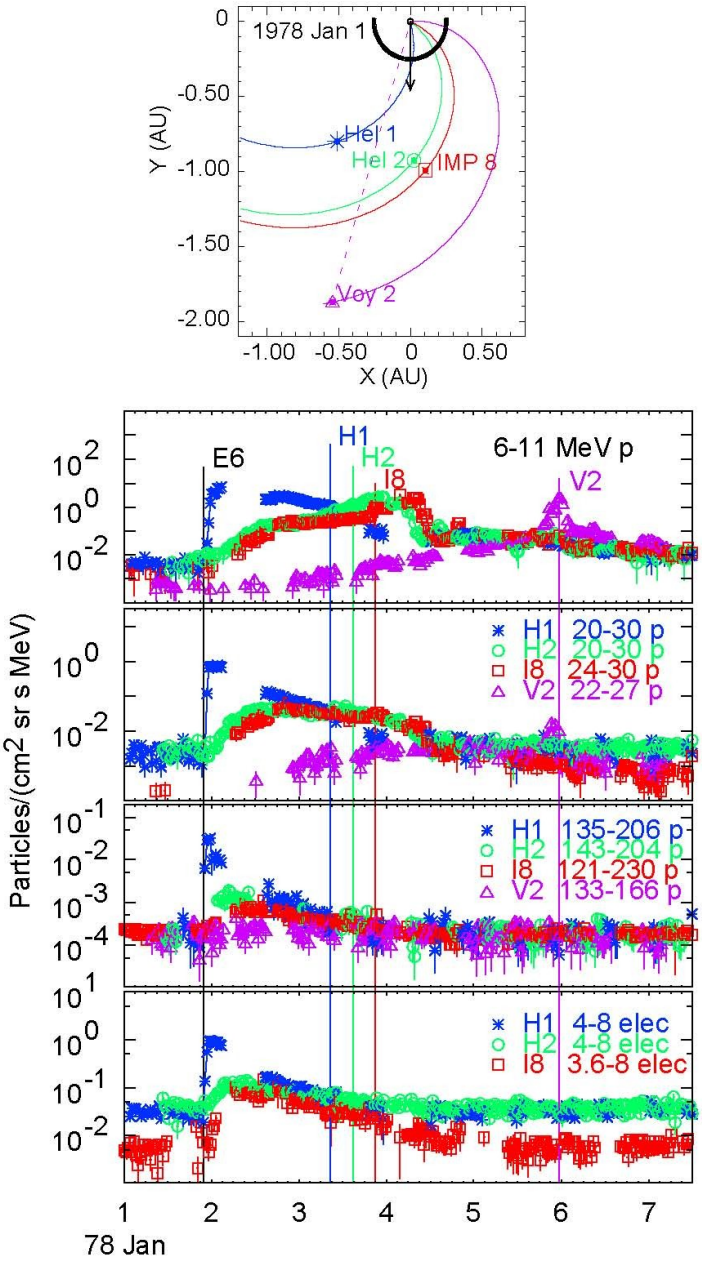

Figure 3. The upper panel shows the configuration of the spacecraft, *Helios 1*, *Helios 2*, IMP 8, and *Voyager2* during the SEP event on January 1, 1978 relative to the CME which is directed downward as shown by the arrow. (*Voyager* 1 is indistinguishably close to *Voyager* 2.) The lower panels compare the intensities of protons and electrons observed on the 4 spacecraft at the energies (in MeV) indicated. Vertical lines show times of shock passage at the spacecraft indicated. Note that the electron intensities after January 4 are higher at *Helios* than IMP 8 only because of higher instrument background; they do not necessarily suggest absence of an electron reservoir.

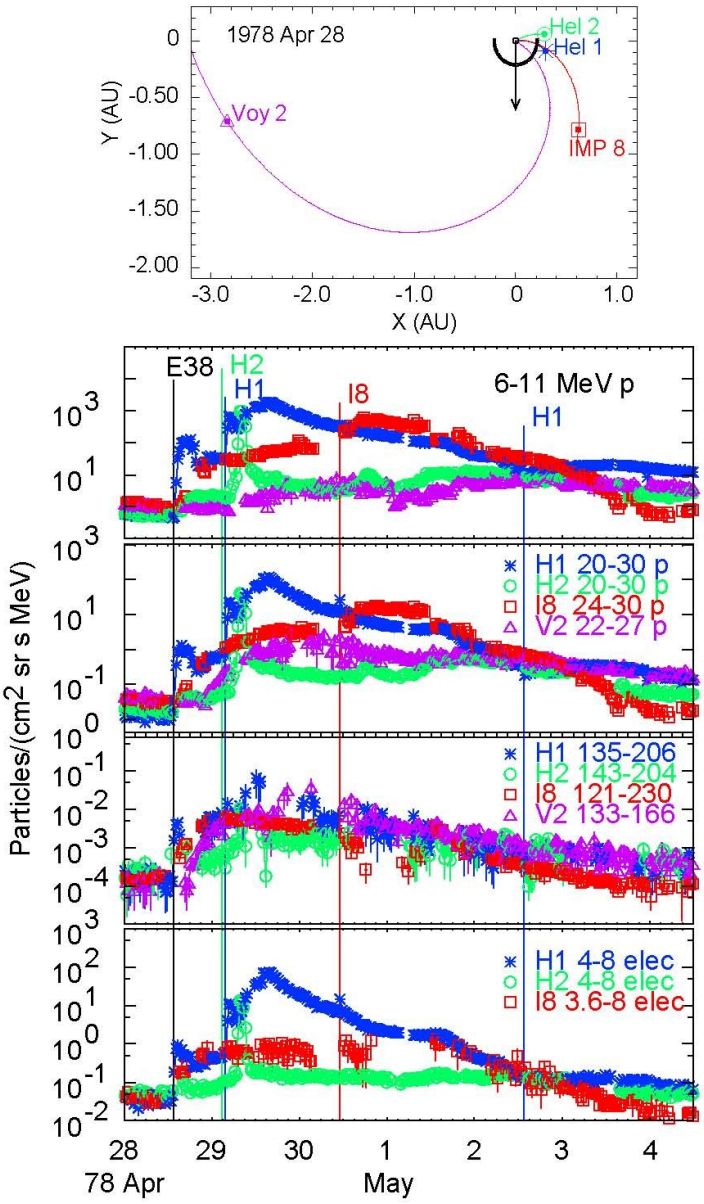

Figure 4. Observations during the event of April 28, 1978 are shown with features as described in Figure 3.

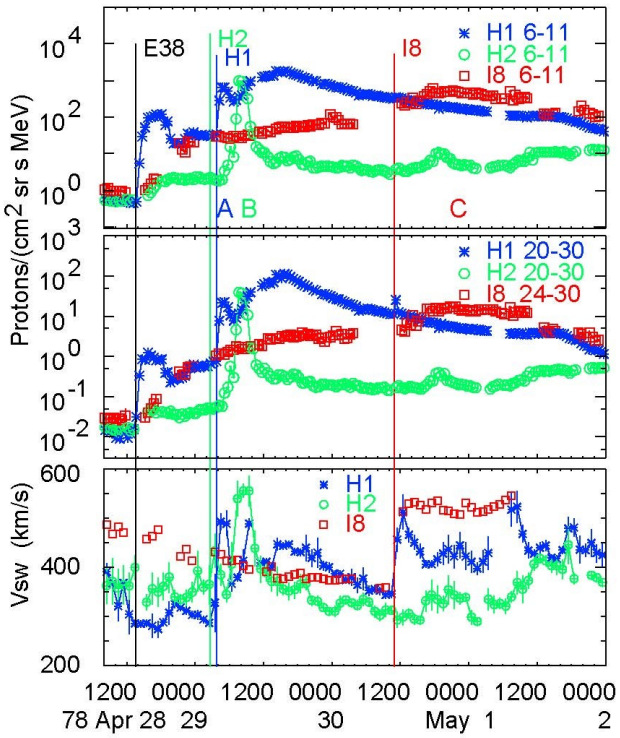

Figure 5. Particle intensities at *Helios 1*, *Helios 2*, and IMP 8 are shown in the upper two panels and compared with the solar wind speed in the lower panel. Peaks in the solar wind speed for the 3 spacecraft correlate with peaks in the corresponding particle intensities at times labeled A, B, and C in the upper panel.

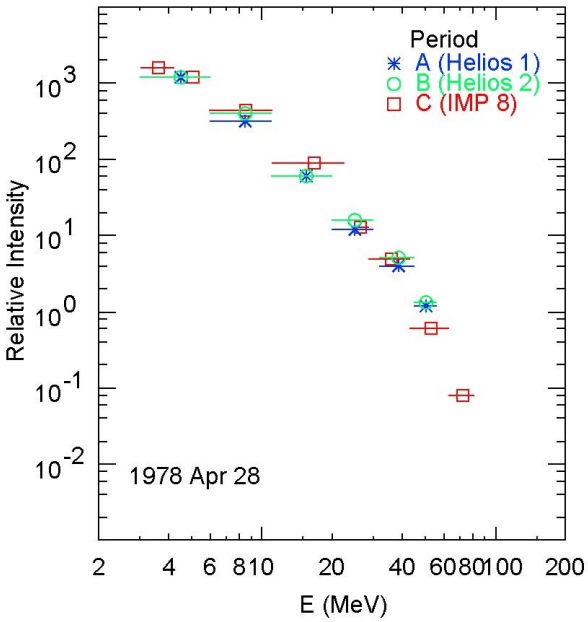

Figure 6. Proton energy spectra are shown during high-speed solar wind periods A, B, and C (marked in Figure 5) at *Helios 1*, *Helios 2*, and IMP 8, respectively.

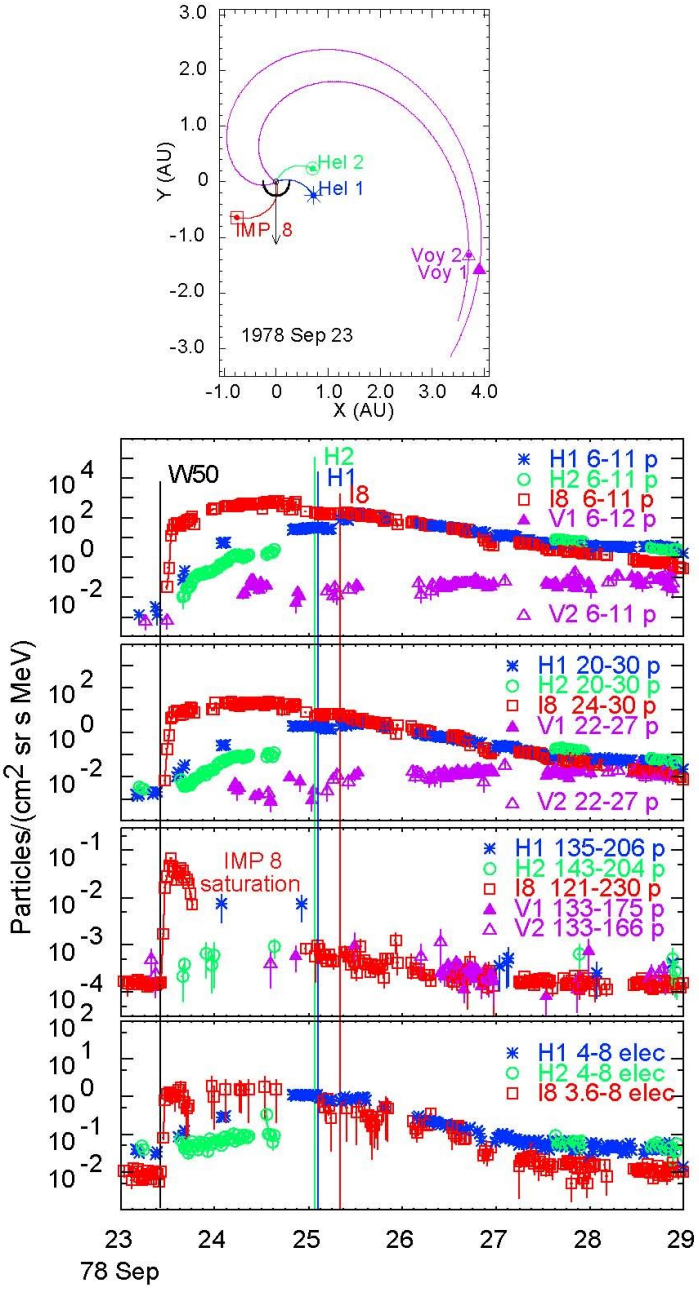

Figure 7. Observations during the event of September 23, 1978 are shown with features as described in Figure 3.

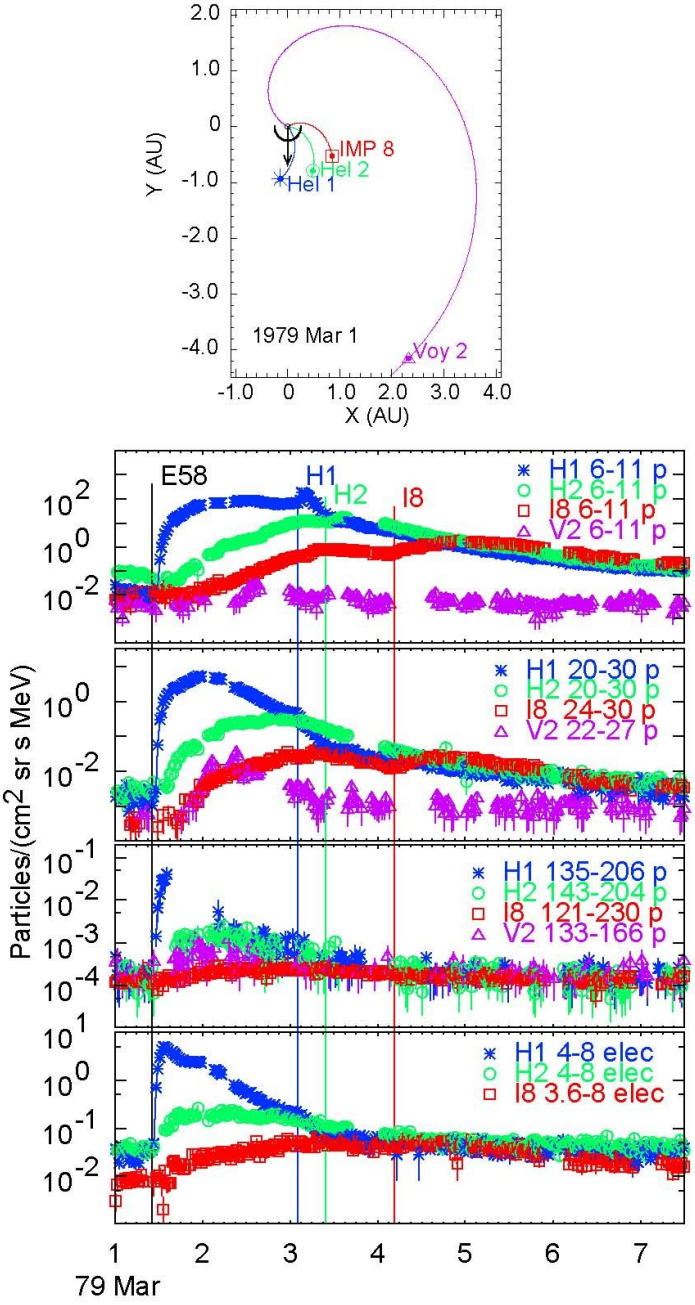

Figure 8. Observations during the event of March 1, 1978 are shown with features as described in Figure 3.

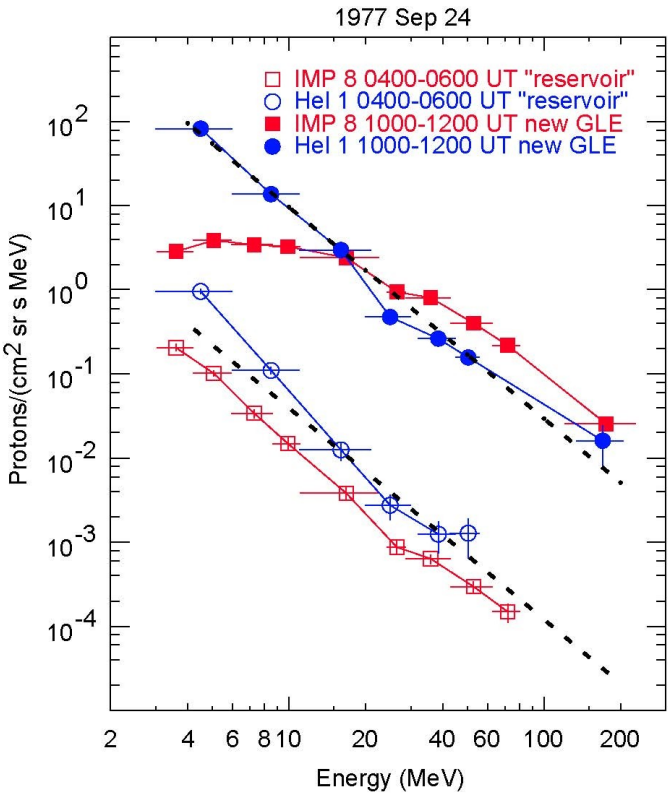

Figure 9. Proton energy spectra at IMP 8 (red squares) and *Helios 1* (blue circles) are compared in the reservoir region prior to the September 24, 1977 GLE (open symbols) and on the plateau region in this new GLE at 10 to 12 UT (closed symbols). The new GLE plateau spectrum at *Helios 1*, fit to a power-law, is shown as a dashed line and is also shown shifted downward for comparison with the reservoir spectra. The plateau spectrum at IMP 8 has a similar slope at high energy but rolls down at low energy.